JOURNAL OF CATALYSIS 154, 345–354 (1995)

Studies on Pt_xSn_y Bimetallics in NaY

I. Preparation and Characterization

P. Mériaudeau,*,[1] C. Naccache,* A. Thangaraj,* C. L. Bianchi,† R. Carli,†
V. Vishvanathan,‡ and S. Narayanan‡

*Institut de Recherches sur la Catalyse, CNRS, 2 avenue A. Einstein, 69626 Villeurbanne Cedex, France; †Universita di Milano, Dipartimento di Chimica Fisica et Electrochimica, Via Golgi 19, 20133 Milan, Italy; and ‡Indian Institute of Chemical Technology, Hyderabad, 500007 India

Received August 22, 1994; revised February 2, 1995

A series of materials containing 1.7 wt% Pt and with Pt/Sn atomic ratios varying from 2.25 to 0.6 were prepared using NaY support. The method used to form PtSn bimetallic is based on the reaction of tetramethyltin with hydrogen covering performed Pt particles. Different techniques such as H_2 chemisorption, CO chemisorption, IR spectroscopy, TEM and STEM–EDX analysis, and XPS were used to characterize these materials. It appears that H_2 and CO chemisorption are depressed with the addition of tin and that part of the tin is alloyed with Pt to form a bimetallic. The bimetallics so formed are rather heterogeneous; neither CO chemisorption and IR spectroscopy nor XPS gives clear evidence of a possible change in the electronic properties of Pt with the addition of tin.

INTRODUCTION

The deactivation of Pt-based catalysts used in reforming and dehydrogenation reactions is generally a fast process. It is known that the addition of elements like Re (1), Sn (2), and In (3) increases the lifespan of the catalysts. The PtSn-based catalyst has been extensively studied, even though it is not the dominant commercial catalyst (4, 5); most of these studies were performed on $PtSn/Al_2O_3$ samples. The salient questions and possible answers are:

—Is Pt alloyed with tin? It has been shown that under reducing conditions, PtSn bimetallic was formed (6, 7, 8, 9) but only part of the tin was alloyed with Pt, the other part being deposited onto the Al_2O_3 support (6); for low tin loading the tin is preferentially located on the support (6, 10). Direct evidence of Sn^0 formation was obtained either by Mössbauer spectroscopy (9) or by XPS (6) and indirect evidence of Sn^0 formation was obtained by TPR and chemisorption studies (9).

—Are the electronic properties of Pt modified by tin addition? There is some difficulty in showing any change in the electronic state of Pt in supported PtSn particles by XPS because the observed shift of Pt4*f* binding energy is only 0.2 eV when Pt is alloyed with Sn; this value is a smaller change than can be detected by XPS. So it appears that on supported PtSn, the electronic effect is rather small, if it exists. Indirect methods, such as IR spectroscopy of adsorbed CO help to provide evidence of changes in the electronic properties of Pt. However, the shift of the Pt–CO singleton vibrator is also dependent on the Pt coordination number and thus on the size of the Pt particles. A small downward shift (5 to 10 cm^{-1}) (11, 12) or a small upward shift (11) of the Pt–CO singleton frequency is reported. In contrast, for Sn/Pt(111) surface alloys, it has been shown that Sn has a substantial electronic effect on the Pt(111) surface chemistry (13).

—What is the role of nonalloyed tin? It has been shown (10, 14) that ionic tin can be adsorbed onto the support and hence change the acidity of the support and consequently can affect coke formation.

Recently, it has been shown that PtSn/silicalite and PtIn/silicalite are excellent dehydrogenation catalysts, showing low deactivation rates in isobutane dehydrogenation (15); model dehydrogenation catalysts, PtInNaY, have been recently described (16) and for comparison PtSnNaY are studied here. To prepare metal or bimetallic particles in zeolite hosts, various methods can be used (17). Here we have chosen to react hydrogen Pt-covered surface with an organometallic tin compound as described, by Margitfalvi *et al.* (18) and by Travers *et al.* (19). According to these authors, the alkytin compound reacts with Pt–H surface entities as follows:

$$Pt\text{–}H + Sn(C_2H_5)_4 \rightarrow PtSn(C_2H_5)_3 + C_2H_6$$

$$PtSn(C_2H_5)_3 + 3/2H_2 \rightarrow PtSn + 3\,C_2H_6.$$

[1] To whom correspondence should be addressed.

0021-9517/95 $12.00

We report on the preparation and the characterization of the catalysts and, in a coming paper, we will describe their catalytic properties in propane dehydrogenation and hydrogenolysis and in the *n*-hexane dehydrocyclisation.

EXPERIMENTAL

All the samples were prepared starting with NaY zeolite from Zeocat (France) as a support. The NaY sample was exchanged overnight with a solution of $Pt(NH_3)_4(OH)_2$ at 80°C, typically 5 g of NaY was stirred in 0.5 liter solution of platinum salt from Johnson Matthey. After having been washed twice with water, the sample was dried in air overnight at 373 K. The platinum loading is of 1.7 wt%, as measured by chemical analysis (atomic absorption spectroscopy).

A portion of the as-prepared fresh sample was then slowly heated under a flow of O_2 (2 liter/hr) with a ramping of 0.2 K/min from room temperature to 573 K and maintained at this temperature for 2 h; then the sample was flushed with N_2 and reduced under H_2 (2 liter/hr), while the temperature was increased from 573 K to 773 K at 1 K/min. After 2 h at 773 K, the temperature was decreased to room temperature and the solid was stored under He. The as-prepared sample was utilised as starting material for preparing tin loaded samples.

Formation of PtSn NaY

In a cell identical to that described in (20) a mixture of *n*-hexane and tetramethyl tin (TMT) was contacted with the sample at RT. The TMT content was varied to obtain different tin loadings. The *n*-hexane and TMT mixture was left overnight in contact with the sample and the liquid phase was removed by evaporation through a vacuum line; the sample was then outgassed, *T* being increased from *RT* to 473 K (ramping 0.5 K/min). After 2 h at 473 K, the sample was flushed with hydrogen and reduced under a flow of H_2 from 473 K to 773 K (ramping 0.5 K/min); after 2 h at 773 K, the sample was flushed with N_2, cooled down to room temperature, and contacted with air. This method of forming Pt Sn (18) or Rh Sn (19) bimetallics has been reported previously. Since after the reaction of the alkytin with the surface the alkyligands are removed under H_2, carbonaceous fragments are removed in the form of alkanes and alkenes (18, 20) and no carbon deposit is formed on the bimetallic surface (see XPS results).

H2 Chemisorption Studies

A volumetric apparatus equipped with a Texas Instrument precision gauge was used to study isotherm adsorption. Before any measurement, the sample was re-reduced under dynamic conditions (H_2 flow, 2 liter/hr) at 773 K for 3 h and cooled down to *RT*. Then a first isotherm was measured and the solid was outgassed for 10 min at *RT* ($P = 10^{-2}$ Pa) before the measurement of a second isotherm. The difference between the first and the second isotherms extrapolated to zero pressure gives the amount of strongly chemisorbed hydrogen, and the dispersion was calculated assuming a stoichiometry $H/Pt_s = 1$.

Transmission Electron Microscopy (TEM) and Scanning Transmission Electron Microscopy–Energy (STEM) Dispersive X-Ray Analysis (EDX)

A few samples were characterised using transmission electron microscopy. Particle sizes were measured from micrographs obtained with a Jeol 2010 TEM, and the composition of the individual particles was studied by using the STEM–EDX technique (VG. HB501 apparatus).

X-Ray Photo-Electron Spectroscopy (XPS)

Some samples have been analysed during a Surface Science Instruments (now Fisons Instruments) XPS spectrometer. Monochromated Al$K\alpha$ radiation (1486.6 eV) was used.

CO Chemisorption Studied by Infrared Spectroscopy

Samples were pressed into thin wafers (15–20 mg), mounted in a special holder, and introduced into an infrared cell, allowing the circulation of gases. The samples were re-reduced under a flow of H_2 at 773 K for 2 h and evacuated at this temperature ($p = 10^{-2}$ Pa) before being cooled down to room temperature and contacted with CO ($p = 0.2$ kPa). The IR spectra were recorded with a Bruker IFS 48 FTIR spectrometer.

RESULTS

Hydrogen Chemisorption

The H/Pt values obtained for different samples are given in Table 1.

It appears that the addition of tin decreases H_2 chemisorption. This could be due to the blocking of Pt surface atoms by tin adduct, a modification of their chemisorption properties, or an increase in particle sizes with the tin addition.

TEM AND STEM–EDX Results

The PtSnNaY samples were analysed by TEM. As indicated in Fig. 1a (PtNaY sample) the Pt particles are quite small, most of them having a diameter in the range 0.8–1.2 nm, very few being larger than 2 nm. These results are in good agreement with the hydrogen chemisorption results. The addition of increasing amounts of tin (Fig. 1, b–d) causes an increase in the particles' sizes. The electron micrographs also showed few large particles. A careful examination shows that the micrographs of these large particles are in fact formed by dark centers surrounded

TABLE 1

H_2 Adsorption at 298 K

Sample[a]	$Pt_{1.7}$	$Pt_{1.7}Sn_{0.75}$	$Pt_{1.7}Sn_{0.9}$	$Pt_{1.7}Sn_{1.4}$	$Pt_{1.7}Sn_{2.4}$
H/Pt	1	0.43	0.38	0.26	0.17

[a] $Pt_{1.7}Sn_y$ (y varying from 0 to 2.4) refers to a sample with 1.7 wt% Pt and y wt% Sn.

by light-dark crowns (see particle indicated by an arrow, Fig. 1d).

STEM–EDX Analysis

Three different types of analysis were performed:

—analysis of large zones (10 μm^2) containing several metallic particles,

—analysis of small zones containing one metallic particle of large diameter (3–6 nm),

—analysis of small zones containing one or few individual particles of less than 2 nm. The results are summarized on Table 2.

Table 2 indicates that the results of the large zone analysis are in reasonable agreement with the results of the chemical analysis. For the lowest tin loading the Pt/Sn ratios obtained from analysis of individual small particles or from analysis of individual large particles are higher than the values obtained through large zone analysis, suggesting that for this low tin loading, part of the tin has reacted with the zeolite surface. For the $Pt_{1.7}Sn_{0.75}NaY$ sample, STEM–EDX analysis has shown also that there exist on the zeolite support few areas where Sn was the only metal detected. The Pt/Sn values measured on individual small particles are higher than those obtained for larger particles; apparently, the large Pt particles exhibit a higher propensity to adsorb TMT as compared with small Pt particles. This could be due either to a higher reactivity of Pt–H towards TMT in the case of large parti-

TABLE 2

STEM Analysis of PtSnNaY Samples

Sample	Nature of the analysis and, in parentheses, number of analyses	Pt/Sn (atomic ratio): highest value, average value, and lowest value	Pt/Sn[a]
$Pt_{1.7}Sn_{0.75}NaY$	Large zones[b] (7)	2.2	2.25
		1.9	
		1.8	
	Individual large particles[c] (9)	4	
		3.7	
		3.6	
	Individual small particles[d] (10)	6	
		5.5	
		5.2	
$Pt_{1.7}Sn_{1.4}NaY$	Large zones (5)	1.6	1.21
		1.4	
		1.3	
	Individual large particles (8)	1.8	
		1.7	
		1.5	
	Individual small particles (11)	3.5	
		3.2	
		3.1	
$Pt_{1.7}Sn_{2.4}NaY$	Large zones (5)	0.8	0.63
		0.6	
		0.5	
	Individual larges particles[e] (8)	0.1	
		0.06	
		0.04	
	Individual small particles (11)	3.4	
		2.9	
		2.7	

[a] Atomic ratio from chemical analysis.
[b] Large zones including a great number of individual particles.
[c] Particles of 3–6 nm (see TEM).
[d] Particles of less than 2 nm.
[e] Particles of 3–20 nm (see TEM, Fig. 1d, arrow).

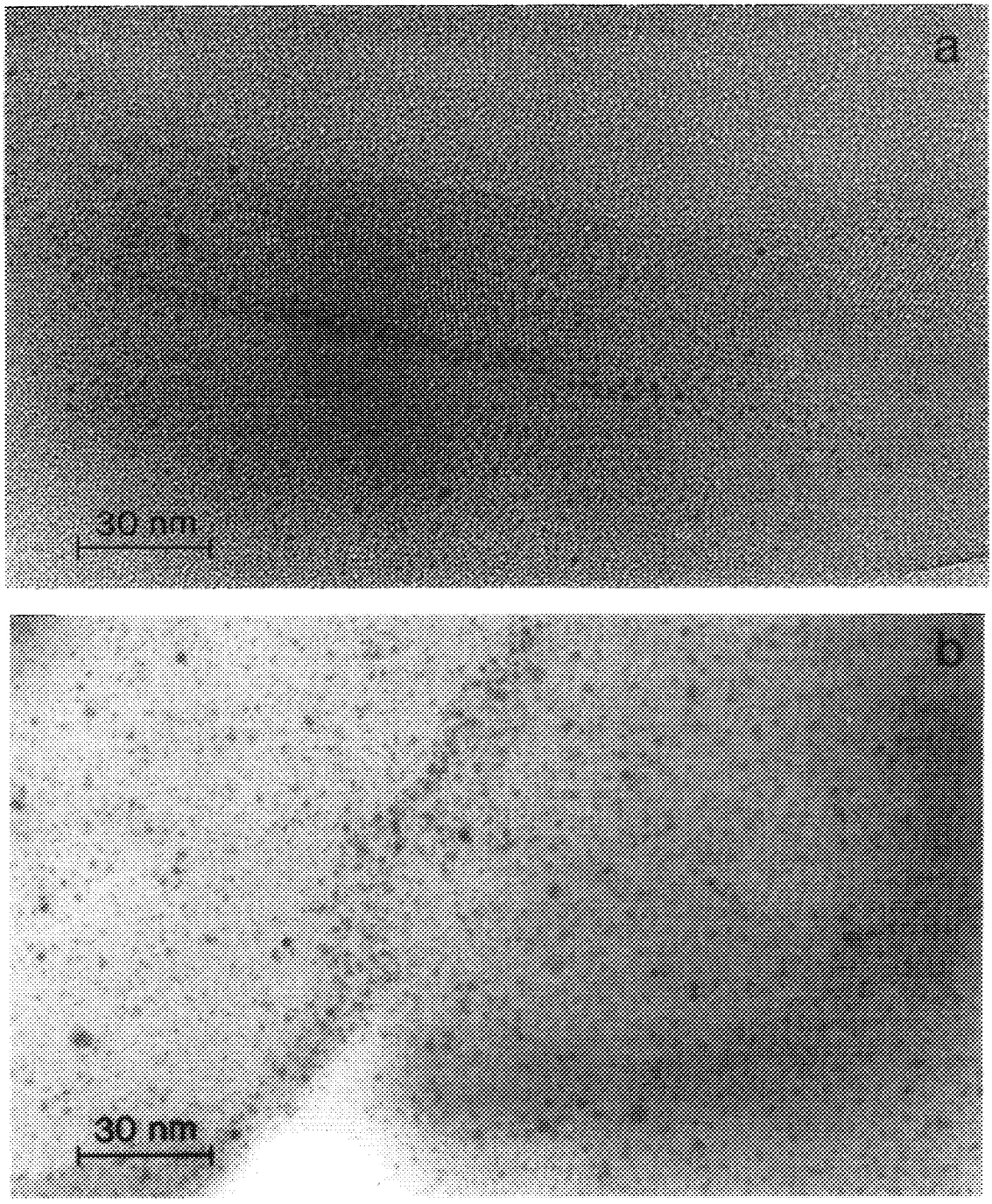

FIG. 1. TEMs of $Pt_{1.7}NaY$ (a), $Pt_{1.7}Sn_{0.7}NaY$ (b), $Pt_{1.7}Sn_{1.4}NaY$ (c), and $Pt_{1.7}Sn_{2.4}NaY$ (d).

cles or to the low diffusion rate of TMT in the zeolite channels: one could reasonably assume that small Pt particles are located within the channels of the zeolite while large Pt particles are deposited on the external surface of the zeolite grains. Thus it is suggested that the diffusion of TMT along the zeolite channels is restricted. The difference in TMT concentration in the zeolite channels and on the zeolite grains should be responsible for the higher tin uptake for those Pt particles located on the external surface. For the sample with the highest tin loading, it is observed that Pt/Sn values obtained for the large particles are lower than the chemical analysis value; careful examination of TEM micrographs (see Fig. 1d, arrow) clearly indicated that these large particles are composed of Pt-

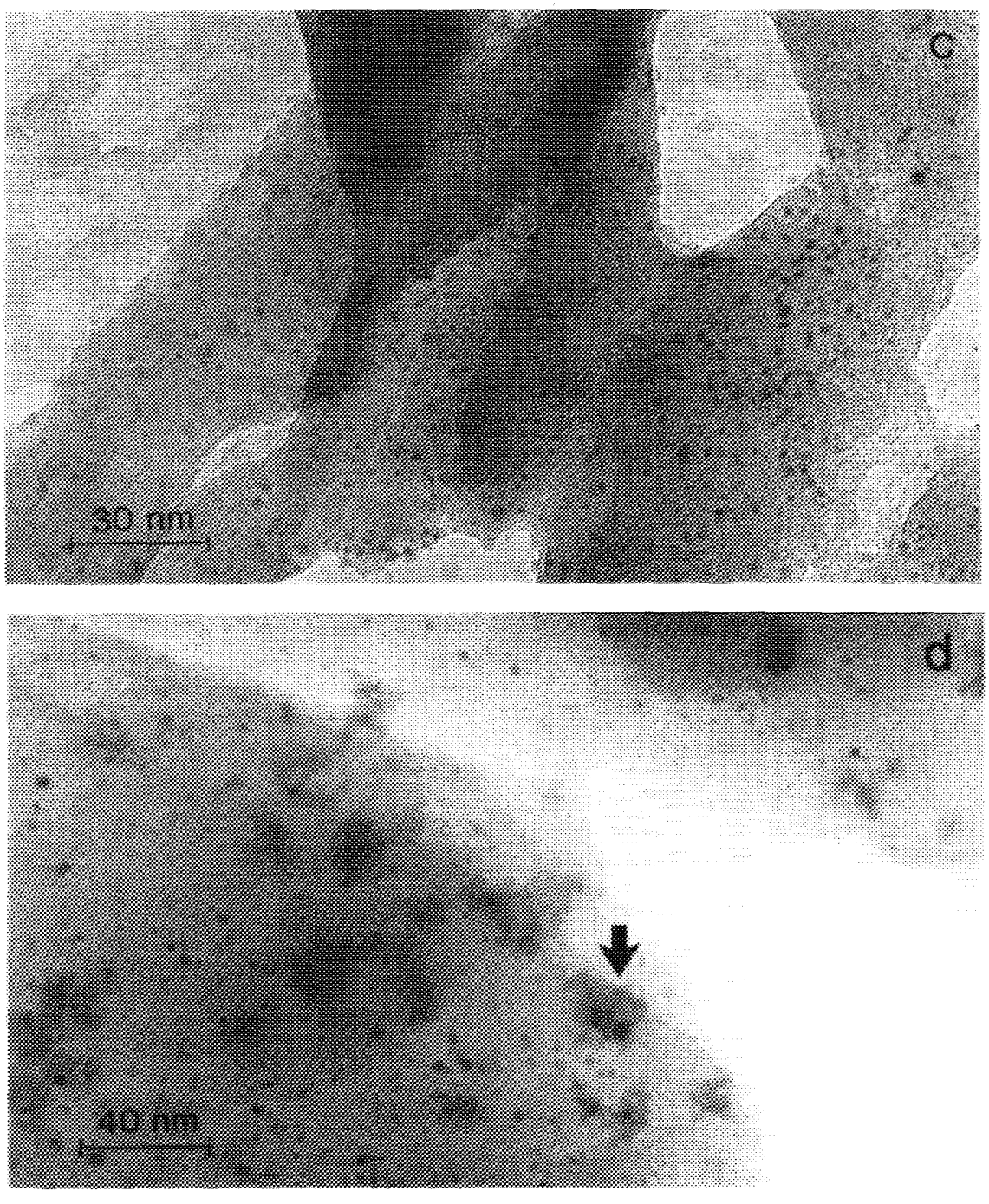

FIG. 1—*Continued*

supported tin (darker zones) and patches of tin (clearer zones) surrounding PtSn particles. Again small particles have Pt/Sn values much higher than that expected from chemical analysis; it has to be noticed that when tin loading is increased from 1.4 wt% to 2.7 wt% the composition of individual small particles remains nearly the same, suggesting that there is a limit in the amount of Sn which can be deposited onto small particles. It is known from TEM that these particles are small (0.8 to 1 nm), and if they are located in the zeolite supercages, the addition of a few Sn atoms would increase the particle diameter to nearly that of the supercage and consequently it would be not possible to add additional tin to these particles.

To summarize, STEM–EDX studies indicate that the tin distribution is rather inhomogeneous. As a general rule, small particles located inside the zeolite cavities

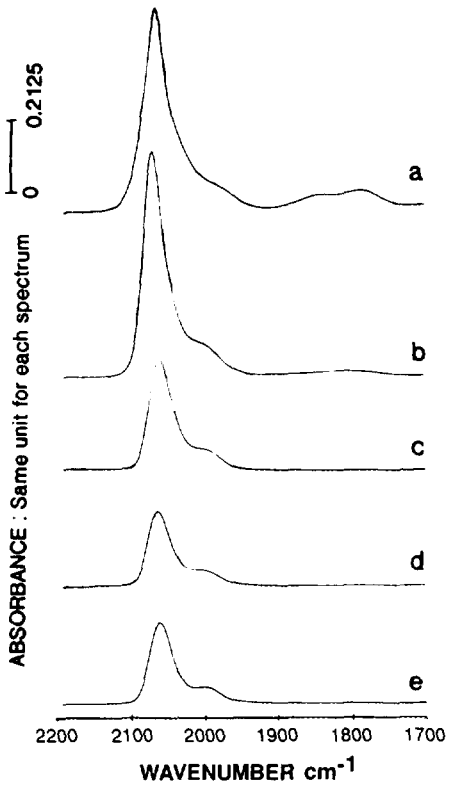

FIG. 2. IR spectra of adsorbed CO on $Pt_{1.7}NaY$ (a), $Pt_{1.7}Sn_{0.7}NaY$ (b), Pt1.7$Sn_{0.9}$NaY (c), $Pt_{1.7}Sn_{1.4}NaY$ (d), and $Pt_{1.7}Sn_{2.4}NaY$ (e).

have a tin content lower than that expected from chemical analysis, but the tin content of these small particles increase with the tin loading up to Pt/Sn values close to 3.

CO Chemisorption as Studied by IR Spectroscopy

Figure 2 reports the IR spectra obtained after the CO was chemisorbed at 298 K (15 min, P_{CO} = 0.5 kPa) and evacuated at 298 K (15 min, P = 0.1 Pa). For the $Pt_{1.7}NaY$ sample, the IR spectrum (Fig. 2a) is composed of two IR bands, one due to the Pt–CO linear vibrator at 2074 cm^{-1}, the other at 1890 cm^{-1} attributed to bridged CO species (21). A weak shoulder (≈2000 cm^{-1}) reveals the presence of other CO species and has recently been attributed to linear Pt–CO perturbed by Na^+ cations or by the zeolite framework (22).

Figure 2, b–e indicates that the addition of tin causes

—a decrease in the linear Pt–CO wavenumber and a decrease in the intensity of this vibration, and

—a stronger decrease in the intensity of the vibration due to bridged CO species.

Table 3 gives the wavenumbers of the different vibrations for full CO coverage and those measured at low CO coverage together with the absorbances of the different vibrations.

From Table 3, three major facts emerge:

—As tin loading is increased, the absorbance of linear and bridged CO decreases, the larger decrease being that of bridged species.

—νCO (linear singleton) at full CO coverage is higher for the PtNaY sample than for the PtSnNaY samples.

—νCO (linear singleton) at low CO coverage is lowest for the PtNaY sample, the addition of Sn causing an upward shift.

XPS Studies

Only three samples were studied by XPS, $Pt_{1.7}NaY$, $Pt_{1.7}Sn_{0.7}NaY$, and $Pt_{1.7}Sn_{1.4}NaY$. XPS spectra were registered on samples that had been outgassed at 723 K (P = 10^{-3} Pa) and on samples reduced *in situ* under H_2 at 723 K (P_{H2} = 101 kPa).

TABLE 3

CO Adsorption over Pt_xSn_yNaY Samples as Studied by IR Spectroscopy

Sample	Absorbance of Pt–CO linear species[a]	Absorbance of bridged CO species[a]	νCO (cm^{-1})		$(A_{523}/A_{298})^d$
			θ^b = 1	θ^c = 0.1	
$Pt_{1.7}NaY$	32	3	2074	2050	0.44
$Pt_{1.7}Sn_{0.7}NaY$	30	0.7	2072	2054	0.25
$Pt_{1.7}Sn_{0.9}NaY$	16	0	2066	2060	0.03
$Pt_{1.7}Sn_{1.4}NaY$	11	0	2064	2060	0.03
$Pt_{1.7}Sn_{2.4}NaY$	11	0	2062	2060	0.04

[a] As measured in Fig. 2.

[b] As measured in Fig. 2.

[c] After having evacuated the sample at 523 K until the absorbance of Pt–CO linear species reaches 1/10 of its initial value as registered after evacuation for 15 min at 298 K.

[d] Absorbance of Pt–CO singleton after evacuation for 15 min at 523 K (A_{523}) divided by absorbance after evacuation for 15 min at 298 K (A_{298}).

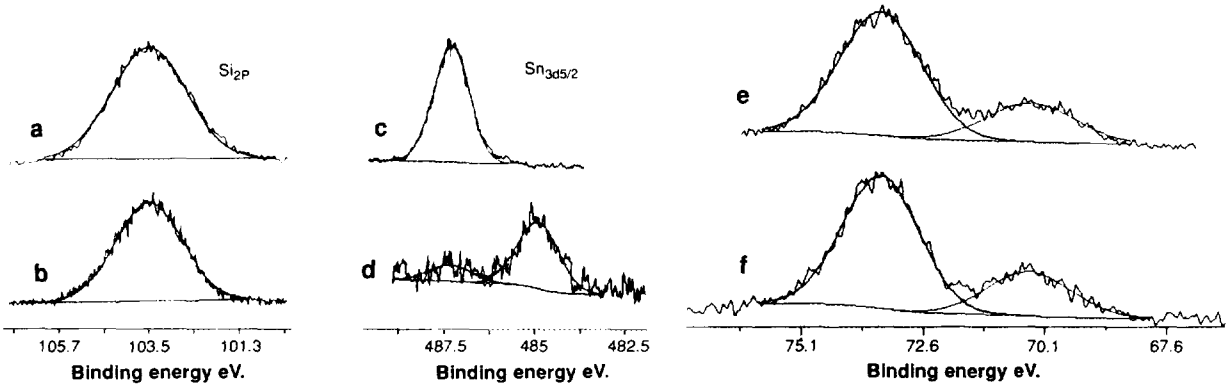

FIG. 3. XPS Si2*p* and Sn3*d* spectra of the $Pt_{1.7}Sn_{0.7}NaY$ sample. Si2p (a) before reduction and (b) after H_2 reduction Sn/3d (c) before reduction and (d) after reduction. Al2*p*Pt4*f* (e) before reduction and (f) after H_2 reduction.

The spectra of Pt4*f*, Sn3*d*, Si2*p*, and Al2*p* were registered, Si2*p* = 103.5 ev being used as an internal reference. The spectra in Fig. 3a–f reflect the $Pt_{1.7}Sn_{0.7}NaY$ sample before and after reduction. Examination of Fig. 3, a and b indicates that the Si2*p* lines are identical (shape is unchanged). By contrast the Sn3*d* lines are greatly modified by reduction; this clearly indicates that there is no inhomogeneous charging effect and by consequence it will be possible to discuss the changes observed in the Sn3*d* line. Figure 3, e–f allows the determination of $Pt4f_{7/2}$ binding energy. In addition to these data, C1*s* spectrum was registered for each sample; after the H_2 *in situ* treatment, the C/Si atomic ratios for Pt_2NaY, $Pt_2Sn_{0.7}NaY$, and $Pt_2Sn_{1.4}NaY$ are 1.1×10^{-3}, 1.3×10^{-3}, and 1.2×10^{-3}, respectively. Table 4 reports Pt/Si, Sn/Si, and Pt/Sn ratios obtained from XPS data using the cross sections tabulated by Scofield; the binding energies (BE) of Pt and Sn measured after different treatments are reported on Table 5.

DISCUSSION

From the TEM results it appears that, as reported earlier, the NaY support allows the formation of small Pt particles, most of them having sizes smaller or equal to 1 nm, in agreement with the chemisorption results. A relatively few number of larger particles are also observed (Fig. 1a) so that, within experimental error, the H_2 chemisorption produced a H/Pt ratio equal to 1.

Adding tin to Pt has several effects and we will discuss the following questions:

—Are the particle sizes modified with the addition of tin?

—Are both elements (Pt and Sn) in the same particle, and if yes, are they forming a bimetallic?

—Are the electronic properties of Pt modified through the addition of tin?

TABLE 4

XPS Data: Pt/Si, Sn/Si, and Sn/Pt Atomic Ratios as a Function of the Thermal Treatment for Different Solids

	Atomic ratio					
	Pt/Si ($\times 10^2$)		Sn/Si ($\times 10^2$)		Pt/Sn	
Sample	by XPS[a]	by EA[b]	by XPS[a]	by EA[b]	by XPS[a]	by EA[b]
$Pt_{1.7}NaY$	0.57	1.2	—	—	—	—
$Pt_{1.7}Sn_{0.7}NaY$	0.5	1.2	1	0.8	0.5	1.4
	(0.46)		(0.6)		(0.76)	
$Pt_{1.7}Sn_{1.4}NaY$	0.28	1.2	3.5	1.6	0.08	0.74
	(0.43)		(0.7)			

[a] Values calculated with XPS data. First number, after evacuation at 723 K; number in parentheses, after reduction in H_2 at 723 K.

[b] As measured by chemical analysis.

TABLE 5

Binding Energies (eV) of Pt and Sn for the Three Samples under Study as a Function of the Thermal Treatment

Sample	Binding energies[a] (eV)	
	Pt4$f_{7/2}$	Sn3$d_{5/2}$
$Pt_{1.7}NaY$	71.8 (71.5)	—
$Pt_{1.7}Sn_{0.7}NaY$	71.6 (71.2)	487.6 484.9[b] 487.6
$Pt_{1.7}Sn_{1.4}NaY$	71.5 (71.25)	487.4 484.90[c] 487.30

Note. Si2p (103.5 eV) has been taken as an internal reference.

[a] After evacuation at 723 K and (in parentheses) after reduction in H_2 at 723 K.

[b] Sn species at 484.9 eV represent 90% of the total Sn.

[c] Sn species at 484.90 eV represent 50% of the total Sn.

Figure 1 clearly indicates that the crystallite size of the metal particles increased upon the addition of tin. In this study, the PtSn particles have been made by depositing Sn from $Sn(CH_3)_4$ in a monolayer and/or in multilayer quantities on a Pt crystallite surface. Upon activation in H_2 cherry-like structure of PtSn or/and a three dimensional Sn island growth on the Pt surface would develop which could be responsible for the metal particle growth observed with TEM. This suggestion is reinforced by the STEM–EDX analysis which has shown that indeed Pt and Sn were simultaneously present in both the small and the large cystallites. For low tin loading, the Pt/Sn ratio for large and small particles is higher than that measured from large zone analysis, suggesting that part of the tin was deposited on the zeolite surface, in agreement with the observation that tin is detected in zones having no Pt particles. This observation and the corresponding explanation are valid for higher tin loadings.

For the highest Sn loadings (1.4 wt% and 2.4 wt%) it is observed that Sn patches (as SnO_x?) are deposited in the vicinity of large Pt particles, rendering difficult the measurement of Pt/Sn values for individual particles. The surprising fact is that for all tin loadings, the Pt/Sn ratio for small particles is higher than that for large particles. Contrary to expectations, the number of Pt surface atoms relative to the total number of Pt atoms is higher for small particles. Two possible explanations for this are proposed:

—The diffusion of TMT along the zeolite channels is restricted and the difference in TMT concentration (larger on the surface of the zeolite grain on which large particles are located and smaller inside the zeolite pores in which small particles are located) should be responsible for the higher tin uptake for those Pt particles located on the external surface.

—The hydrogen chemisorbed on large particles has a higher reactivity towards TMT than the hydrogen on small particles.

As pointed out in the introduction, the TMT compound is reacting with Pt–H groups through the sequence

$$Pt\text{–}H + Sn(CH_3)_4 \rightarrow Pt\text{–}Sn(CH_3)_3 + CH_4,$$

the reduction under hydrogen giving PtSn via (18)

$$Pt\text{–}Sn(CH_3)_3 + 3/2H_2 \rightarrow PtSn + 3CH_4$$

For the deposition of tin on the zeolite, as it is evidenced by STEM–EDX analysis it is likely that the tin deposit is occuring via (33)

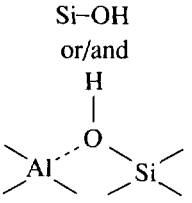

$$+ Sn(CH_3)_4 \longrightarrow Si\text{–}O\text{–}Sn(CH_3)_3 + CH_4$$

$$\xrightarrow{+ 3/2H_2} Si\text{–}O\text{–}Sn + 3CH_4,$$

the reactive OH groups being either silanol groups, as reported in (18), or protons created through the exchange and reduction of platinum ions in NaY via

$$2Na^+/Zeol. + Pt^{2+} \rightarrow Pt^{2+}\ zeol. + 2Na^+$$

$$Pt^{2+}/Zeol. + H_2 \rightarrow Pt/Zeol. + 2H^+/Zeol.$$

Results from Table 1 indicate that the H_2 uptake decreased following the deposition of tin on the Pt crystallite surface; if one assumes that the stoichiometry of hydrogen chemisorption $H/Pt_s = 1$ does not change with Sn addition the metal particle size growth and the surface enrichment with Sn can be seen as responsible for the decrease in the amount of H_2 that is chemisorbed. Assuming that the CO extinction coefficient is independent of the tin loading, the observed pronounced decrease in the total adsorbed amount of CO, derived for the IR band intensities of adsorbed CO, accounts for the growth in particle size and for the enrichment of the PT surface with Sn, this being in qualitative agreement with H_2 chemisorption results.

Another point of discussion concerns the shift in νCO and the relative intensity changes in the IR bands due to linear and bridge CO forms. The IR results showed that the multibonded bridge form decreased more rapidly that the monobonded form. The more pronounced influence

of Sn on multibonded CO suggests that Sn and Pt form bimetallic PtSn, which results in a dilution effect of Pt in Sn, in agreement with previous works on Pt-based bimetallic catalysts (23). For PtSn samples, the νCO (singleton wave number) shifts to a lower wavenumber at full CO coverage, which is considered an indirect proof of the dilution effect, indicating that CO vibrators are much less perturbed by the dipolar effect of the neighbouring adsorbed CO because of the presence of tin. It is of interest that at low coverage ($\theta \rightarrow$ O) the Pt–CO singleton vibrates at higher wavenumbers for PtSn samples than for the pure Pt sample. This shift, attributed to the presence of tin, is not large but clearly evidenced and it has been confirmed by using ^{12}CO ^{13}CO mixtures, owing the progressive decrease of the dipole–dipole interaction (experimental results are not reported here). It could be expected that the TPD of CO should confirm that CO is desorbed at lower temperatures for PtSnNaY than for PtNaY. This is exactly the result reported in Table 3 (last column).

These observations are in line with those reported by Kogan *et al.* (24) for $PtSn/Al_2O_3$ or by Paffett *et al.* (25) for Sn/Pt(111) surface alloys. By contrast, there are some other reports indicating that there is no shift in the Pt–CO singleton upon addition of Sn on Pt-supported Al_2O_3 (11) or that there is a downward shift (12). As pointed out recently (6) the formation of PtSn bimetallic supported on Al_2O_3 depends greatly on the nature of the alumina and on the Sn loading since a part of the tin directly interacts with alumina, and this could explain the contradictory results reported in the literature.

Here, the observed positive shift in the Pt–CO linear singleton with the addition of Sn could be due either to a change in Pt electronic properties or to a particle growth effect, which with an increase in the coordination number of the surface platinum atoms causes shift in the CO band (11, 26) at high frequencies. Since Sn is expected to donate charge to Pt, and consequently should induce a downward shift of CO singleton frequency, the positive shift observed here should indicate that the particle size effect is larger than the electronic effect, if it exists.

These results are at variance with those obtained for PtInNaY (16), for which it has been observed that the Pt–CO bond strength (as measured by TPD) is higher for PtInNaY than for PtNaY, the νCO wavenumber being lower for In-containing samples. Since PtSnNaY bimetallic particles are larger than PtInNaY bimetallic particles, and since similar electronic effects can be expected for Pt in PtSn or PtIn samples, the different behaviours observed with the CO probe suggest that the size effects play a determining role.

Having established how CO chemisorption is modified by the addition of tin, we will now discuss the states of platinum and tin.

However, before this discussion, a few words need to be said on the possible contamination of the Pt surface due the method used to synthesise these bimetallics. This point has not been discussed in previous studies (18, 19, 20) but since demethylation reactions are occurring during the reaction of tin with Pt–H, some carbon could poison the Pt surface atoms and could play a role in the decrease in H_2 or CO chemisorption (see previous section). XPS studies have shown that the C/Si atomic ratios are nearly the same for all the samples under study, showing that the reaction of TMT with Pt–H species and the subsequent demethylation under H_2 is not producing large amounts of carbonaceous deposits on the different solids.

From the XPS data (see Table 5) it is rather difficult to determine if there is a change in the electronic properties of Pt since the binding energy shift (negative) is of 0.2 eV when PtNaY and PtSnNaY are compared. Since particle growth is observed for PtSn samples, this could well induce a change in relaxation effects and by consequence would modify the Pt 4f binding energy. The literature related to this question is rather ambiguous since Balakrishnam *et al.* (27) reported a negative shift in Pt binding energy due to the addition of tin precursor containing no chlorine and a positive shift with chlorinated tin precursor. A small negative shift was observed when comparing Pt and Pt_3Sn alloy (Δ = 0.3 eV) and a positive shift (Δ = 0.2 eV) was observed for Pt and PtSn alloy (28). The reported XPS studies on Sn/Pt(111) are not of great help in solving our problem since the experiments were generally not performed with an apparatus with angle-resolved photoemission, which is a prerequisite for estimating, with this technique, the shift in the binding energy of the Pt surface atoms (29, 30); nevertheless, other spectroscopy studies performed on these model systems indicated that Sn has a substanial electronic effect on Pt(111) surface chemistry (25, 31).

State of Sn and Possible Nature of Pt_x Sn_y Alloy

Concerning the tin state, the XPS data clearly indicate that part of the tin is reduced to Sn^0 (the binding energy of $Sn3d_{5/2}$ is 484.8 eV, compared to 484.9 eV for Sn metal (28)).

Assuming that all Sn^0 is within the bimetallic phase, Tables 4 and 5 allow the calculation of Pt/Sn^0. The atomic ratios Pt/Sn^0 = 1.4 for the $Pt_{1.7}Sn_{1.4}NaY$ sample and Pt/Sn^0 = 1.5 for the $Pt_{1.7}Sn_{0.7}NaY$ samples were obtained. These ratios are different from those obtained by STEM–EDX when focusing the analysis on small particles, probably because XPS, which is a surface technique, reflects more the composition of the large particles located on the external surface of the zeolite grain than that of the small particles located inside the zeolite channels. Due to the heterogeneous distribution of tin, it is impossible to deduce from XPS data any stoichiometry for the bimetal-

lic phases formed. XPS indicates that together with Sn^0, some oxidized tin is present (binding energy at 487.3 eV), the oxidized phase being favoured at high tin loadings (Table 5). It is difficult to discriminate between Sn^{2+} and Sn^{4+} with XPS since their binding energies are very close. Since numerous Mössbauer studies (32, 9) indicated the presence of Sn^{2+} in $PtSn/Al_2O_3$, it is likely that our samples also contain Sn^{2+}, but the presence of Sn^{4+} cannot be excluded.

CONCLUSIONS

To summarize, these studies indicate that the addition of tin to PtNaY samples and the subsequent activation lead to the formation of PtSn particles.

Chemisorption of hydrogen is more depressed by the addition of tin than was CO chemisorption. In both cases, the amount of gas chemisorbed decreased with increasing amounts of tin. TEM and STEM–EDX analyses indicate that bimetallic particles are formed and are Pt enriched. With the addition of tin, particle growth is observed, in agreement with CO chemisorption results. From XPS, it is observed that only a part of the tin is in the Sn^0 oxidation state, the other part being in the Sn^{2+} oxidation state, and not in interaction with Pt. Neither XPS results nor IR results give clear evidence of a change in the electronic properties of Pt with the addition of tin.

ACKNOWLEDGMENTS

Mr. Nicot is acknowledged for having performed TEM– and STEM–EDX analyses. The Indo–French Center for the Promotion of Advanced Research (IFCPAR), New Delhi, India, is acknowledged for funding Project 506-1.

REFERENCES

1. Jacobson, R. L., Kluhsdohl, H. E., McCoy, C. S., and Davis, R. W., *Proc. Am. Pet. Inst. Div. Refin.* 504 (1969).
2. Sinfelt, J., "Bimetallic Catalysts." Wiley, New York, 1983.
3. Imai, T., U.S. Patent 4,886,928 (1989).
4. Srinivasan, R., and Davis, B. H., *Platinum Met. Rev.* **36,** 151 (1992).
5. Dautzenberg, F. N., Helle, J. N., Biloen, P., and Sachtler, W. M. H., *J. Catal.* **63** 119 (1980).
6. Srinivasan, R., and Davis, B. H., *J. Mol. Cat.* **88,** 343 (1994) and references to works by Davis, B. H., therein.
7. Lieske, H., Sarkany, A., and Völter, J., *Appl. Catal.* **30,** 69 (1987) and references to other works by these authors therein.
8. Burch, R., *J. Catal.* **71,** 348 (1981).
9. Hobson, M. C., Goresh, S. L., and Khore, G. P., *J. Catal.* **142,** 641 (1993).
10. Beltramini, J., and Trimm, D. L., *Appl. Catal.* **32,** 71 (1987).
11. Balakrishnan, K., and Schwank, J., *J. Catal.* **138,** 491 (1992).
12. Palazov, A., Bonev, C. H., Shopov, D., Lietz, G., Sarkany, A., and Völter, J., *J. Catal.* **103,** 249 (1987).
13. Xu, C., Tsai, Y. L., Koel, B. E., *J. Phys. Chem.* **98,** 585 (1994).
14. Coq, B., and Figueras, F., *J. Catal.* **85,** 197 (1984).
15. Barri, S., European Patent 0351 066 (1989).
16. Mériaudeau, P., Thangaraj, A., Carli, R., Bianchi, C. L., Narayanau, S., and Naccache, C., *J. Catal.*, **152,** 313 (1995).
17. Sachtler, W. M. H., and Zhang, Z., *Adv. Catal.* **39,** 129 (1993).
18. Margitfalvi, J. L., Hegedus, M., and Tálas, E., *J. Mol. Catal.* **51,** 279 (1989).
19. Travers, C., Burnonville, J. P., and Martino, G., *in* "Proceedings, 8th International Congress on Catalysis, Berlin, 1984," Vol. 4, p. 891. Dechema, Frankfurt-am-Main, 1984.
20. Agnelli, M., Louessard, P., El Mansour, A., Candy, J. P., Burnonville, J. P., and Basset, J. M., *Catal. Today* **6,** 63 (1989).
21. Eischens, R. P., and Pliskin, W. A., *Adv. Catal.* **10,** 2 (1958).
22. Lane, G. S., Miller, J. T., Modica, F. S., and Barr, M. K., *J. Catal.* **141,** 465 (1993).
23. Tooleraar, F. J. C., Stoop, F., and Ponec, V., *J. Catal.* **82,** 1 (1983).
24. Kogan, S. B., Podkletnova, N. M., Oranskaya, O. M., Semenokaya, I. V., and Bursian, N. R., *Kinet. Katal.* **22**(3), 663 (1981).
25. Paffett, M. T., Gebhard, S. C., Windhan, R. G., Koel, B. E., *J. Phys. Chem.* **94,** 6831 (1990).
26. Kustov, L. M., Ostgard, D. J., and Sachtler, W. M. H., *Catal. Lett.* **9,** 121 (1991).
27. Balakrisknan, K., and Schwank, J., *J. Catal.* **127,** 287 (1991).
28. Bouwman, R., and Biloen, P., *Anal. Chem.* **46,** 4044 (1974).
29. Paffett, M. T., Windham, R. G., *Surf. Sci.* **34,** 208 (1989).
30. Hoflund, G. B., Asbury, D. A., Kirszensztejn, P., and Laitenen, H. A., *Surf. Sci.* **161,** L583 (1985).
31. Xu, C., and Koel, B. E., *Surf. Sci. Lett.* **304,** L505 (1994).
32. Li, Y. X., Klabunde, X. J., and Davis, B. H., *J. Catal.* **128,** 1 (1991).